

Excess ellipticity of hot and cold spots in the WMAP data?

Eirik Berntsen

*Institute of Theoretical Astrophysics, University of Oslo, P.O. Box 1029
Blindern, N-0315 Oslo, Norway*

baardeb@astro.uio.no

Frode K. Hansen

*Institute of Theoretical Astrophysics, University of Oslo, P.O. Box 1029
Blindern, N-0315 Oslo, Norway*

frodekh@astro.uio.no

ABSTRACT

We investigate claims of excess ellipticity of hot and cold spots in the WMAP data (Gurzadyan et al. 2005, 2007). Using the cosmic microwave background data from 7 years of observations by the WMAP satellite, we find, contrary to previous claims of a 10σ detection of excess ellipticity in the 3-year data, that the ellipticity of hot and cold spots are perfectly consistent with simulated CMB maps based on the concordance cosmology. We further test for excess obliquity and excess skewness/kurtosis of ellipticity and obliquity and find the WMAP7 data consistent with Gaussian simulated maps.

Subject headings: (cosmology:) cosmic microwave background — cosmology: observations — methods: data analysis — methods: statistical — ellipticity

1. Introduction

Ever since the discovery of the cosmic microwave background (CMB) fluctuations in 1992 (Smoot et al. 1992) the availability and quality of CMB data have been steadily increasing through a series of experiments. The *Wilkinson Microwave Anisotropy Probe (WMAP)* (Bennett et al. 2003) with its most recent seven year maps (Hinshaw et al. 2009) is currently the most important publicly available data set for the study of CMB fluctuations. In the standard model of cosmology the universe is asymptotically isotropic and homogeneous on large scales and the CMB consists of Gaussian fluctuations making the fluctuation *amplitude* on different scales the only relevant information contained in the map.

Studies of CMB fluctuations have classically concentrated on this; achieved most commonly by the transformation of the map to spherical harmonic space and averaging over the directional modes to create the angular power spectrum. The power spectrum, while computationally more forgiving to work with than the original map, is only free of degeneracies under the assumption of perfect Gaussianity and isotropy.

In this paper we will study a property of CMB fluctuations directly related to the map, namely the ellipticity of hot and cold spots. The aim of this study is to follow up on direct measures of ellipticity of spots in CMB data in Gurzadyan et al. (2003a, 2005a, 2003b, 2005b, 2007) where a significant deviation from the ellipticity expected for Gaussian fluctuations was found. It has been shown that within curvature differences of $\Delta\Omega_{\text{tot}} = 0.05$, standard cosmological models produce undetectably small effects in CMB ellipticity compared to a perfectly flat universe (Aurich et al. 2010), so that any excess ellipticity found in *WMAP* would be a significant indication of non-standard physics. For a more complete discussion, see Aurich et al. (2010).

We perform our own analysis of ellipticity on the *WMAP* 7-year data and compare to results stated in the given references, in particular we wish to test the claims of significantly higher ellipticity in *WMAP* data than in simulations and the claims for higher ellipticity on smaller scales. It is also claimed

that there is no evidence of a preferred direction of the spot elongations and we investigate this by obliquity measures of the CMB data.

In §2 we describe the data and masks used in the analysis. The methods used to assess the ellipticity and obliquity are outlined in §3. In §4 we show the results of the ellipticity and obliquity tests applied to the 7-year WMAP data and in §6 we conclude.

2. Data

The analysis in this paper was performed using the seven year release of the WMAP data (publicly available at the Lambda web site¹) as well as a statistical ensemble of 5000 simulated maps of each of the channels Q (41GHz), V (61GHz) and W (94GHz) (the map for each channel is obtained by taking the mean of all differencing assemblies for the given channel). All analysis are performed on either the Q band or the co-added V+W band maps.

From all maps, we have subtracted the best fit mono- and dipole. The mask used throughout was the WMAP KQ85 galactic and point source mask leaving a sky fraction of 82%. Maps were simulated using WMAP noise and beam properties. All maps were pixelized in the HEALPix scheme² (Gorski et al. 2005)

3. Methodology

As described in Gurzadyan et al. (2003a) the method of extracting anisotropic areas is to consider as relevant only those pixels which temperature value is above (or below) a given temperature threshold and as non relevant all pixels which temperature value is below (above) the threshold. A “spot” is then defined to be any set of relevant pixels such that

¹<http://lambda.gsfc.nasa.gov/>

²<http://healpix.jpl.nasa.gov/>

1. any pixel in the set may be path connected on the HEALPix map with any other within the set without moving through a non relevant pixel
2. no pixel in the set may be path connected on the map with a relevant pixel outside the set without moving through a non relevant pixel.

Connectedness is allowed on the diagonal, so that two relevant pixels sharing only a vertex are still connected. The ellipticity measures procedure differs slightly from the one described in Gurzadyan et al. (2003a). Ellipticity for a spot as shown on 1 is measured directly on the sphere with the following algorithm:

1. Double the map N_{side} .
2. Determine the two pixels in the spot, A_1 and A_2 , with the greatest angular distance between them, half of this angular distance is the semi major axis a .
3. Determine the shortest angular distance to this axis for all pixels in the spot. The two pixels (on either side) with the largest distance to the axis are referred to as B_1 and B_2 and their angular distance to the major axis as b_1 and b_2 respectively.
4. The minor axis b is then defined as

$$b = b_1 + b_2 \tag{1}$$

5. Calculate ellipticity, defined as

$$\epsilon \equiv \frac{a}{b}. \tag{2}$$

6. Calculate the obliquity ε , defined as the smallest angle between the great circle traced by the major axis and a chosen equator.

The first step is a purely computational one made to avoid cases where all pixels in a spot fall on a line, causing a potentially near infinite ellipticity as

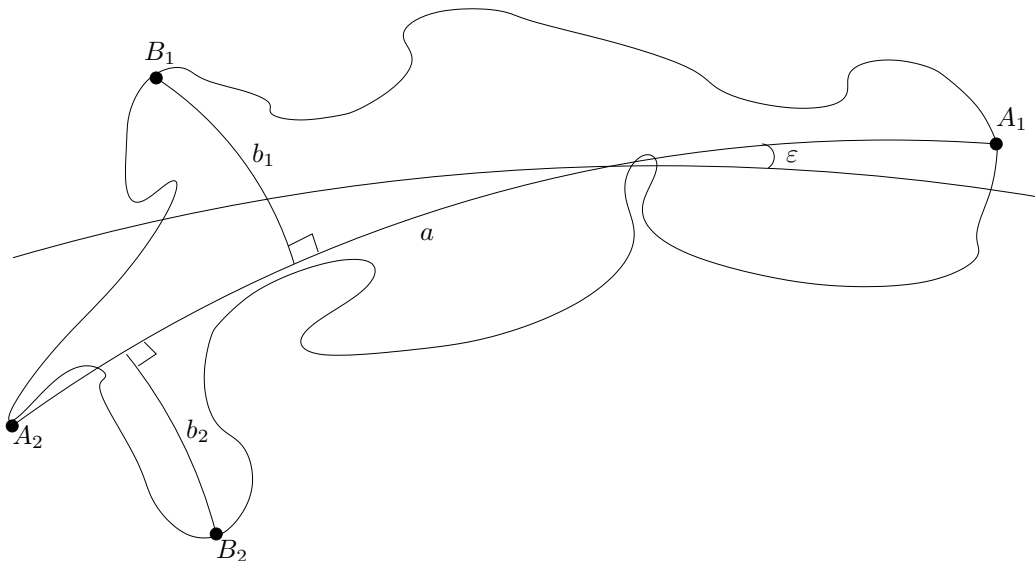


Fig. 1.— Example of a spot (presumably with very high resolution). The major axis is formed between the two points furthest from each other, A_1 and A_2 . The smallest angle ϵ to the equator (the line with no connecting points crossing the figure, so this is an equatorial spot) is the obliquity. The point B_1 is the furthest from the major axis on one side, the point B_2 on the other side.

all pixels return close to zero distance to the major axis. This was seen as superior to the use of vertex positions as a means for less skewed results for smaller spots. Note that any of the three geodesics a , b_1 and b_2 may trace areas not covered by the spot as the major axis does in figure 1. Except for a test of obliquity measures against 12288 chosen equators to check for differences, obliquity was measured against galactic equator. Step 6 differs from Gurzadyan et al. (2003a), as it only measures obliquity from 0 – 90 degrees to avoid ambiguity on polar spots. Finally the results for one map is returned as the average over all spots and statistical uncertainties with no weighting with regard to position or size except that spots smaller than certain values are excluded from some of the analysis. Statistical analysis is carried out in frequentist manner to obtain mean, variance, skewness and

kurtosis

To obtain a result against which to compare the ellipticity and obliquity values of the *WMAP* maps; an ensemble of 5000 maps were simulated using modules included in the HEALPix package. The analysis was performed on simulated and *WMAP* data in the Q, and combined VW bands with thresholds ranging from $-500\mu\text{K}$ to $-40\mu\text{K}$ for negatively defined spots and then from positive $40\mu\text{K}$ to $500\mu\text{K}$ at every 20th μK . The ellipticity and obliquity was calculated for

1. All spots (including the ones with only two pixels).
2. Spots with > 2 pixels.
3. Spots with > 3 pixels.
4. Spots with > 8 pixels.
5. Spots with > 20 pixels.
6. Spots with > 50 pixels.
7. Spots with > 100 pixels.
8. Spots with > 300 pixels.

Single pixel “spots” were ignored throughout.

In order to evaluate the significance of the results, we performed a χ^2 test,

$$\chi^2 = \sum_{tp} \sum_{t'p'} (x_{tp} - \langle x_{tp} \rangle) C_{tp,t'p'}^{-1} (x_{t'p'} - \langle x_{t'p'} \rangle) \quad (3)$$

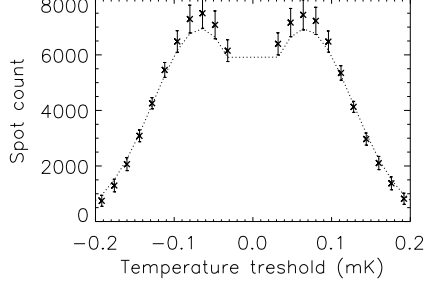
where x_{tp} is the value (mean over all spots for that map) for the ellipticity or obliquity for the map to be tested at a temperature threshold t and for a pixel size p . $\langle x_{tp} \rangle$ is the mean over all simulated maps and $C_{tp,t'p'}$ is the covariance matrix obtained from gaussian simulations based on the WMAP best fit power spectrum and noise model.

4. Results

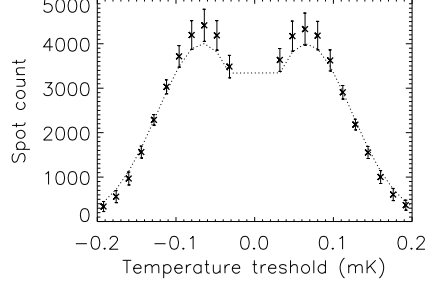
Results gathered for the V+W map is shown in figure 2 (for number of spots) and figure 3 (ellipticity). We do not show plots for the Q band as they are very similar to the VW results. The mean ellipticity value for spots in a perfectly Gaussian map with infinite resolution can be shown to be $\varepsilon \approx 1.648$ (Aurich et al. 2010), so this is the naively expected result. Ellipticity significantly in excess of this number is only evident for spots smaller than 8 pixels, for larger spots, the ellipticity is close to the theoretical value. This is due to a higher probability for smaller spots of consisting only of pixels placed vertically, horizontally or diagonally on a row, resulting in such spots having ellipticity in excess of 10, and hence skewing the results towards a higher mean ellipticity.

Figure 4 shows a map of the spots found in the case of the V+W map with a $+100\mu\text{K}$ threshold. The spots have been color coded to highlight their ellipticity in the range from 1 to 4 with zero (dark blue) representing non-relevant pixels.

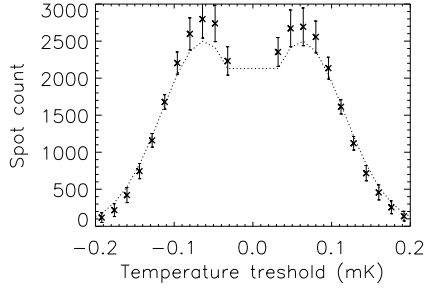
The measured ellipticity and obliquity was compared to an ensemble of 5000 simulated Gaussian maps and values compared to its χ^2 distribution, results for which are shown in table 1 (VW data) and table 2 (Q data). In table 3 we show the total χ^2 summed also over all pixel numbers for ellipticity and obliquity as well as the skewness and kurtosis of these. No significant detection of excess ellipticity could be found for any of the tested bands. In addition to the obliquity measured for the galactic equator, we also measured obliquity against a set of different equatorial rings orthogonal to vectors pointing at the center of all pixels on a $N_{\text{side}} = 32$ map, but still no particular direction or obliquity was found.



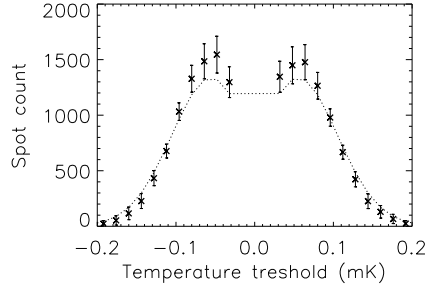
(a) > 3 pixel spots



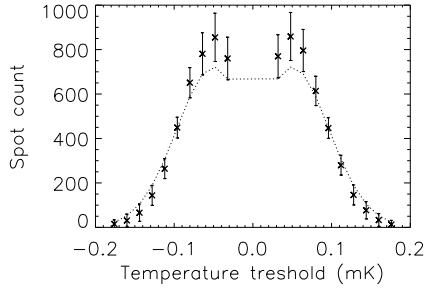
(b) > 8 pixel spots



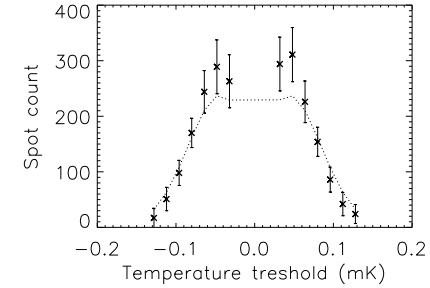
(c) > 20 pixel spots



(d) > 50 pixel spots

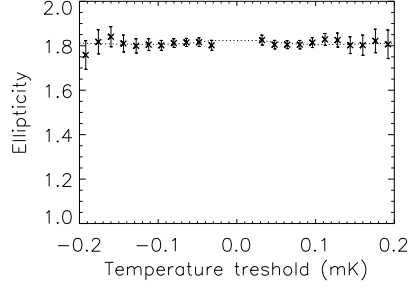


(e) > 100 pixel spots

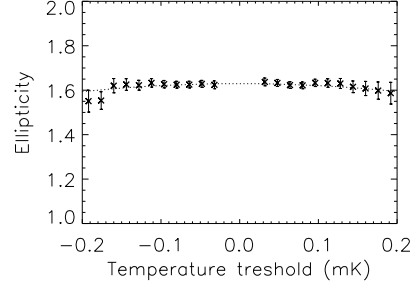


(f) > 300 pixel spots

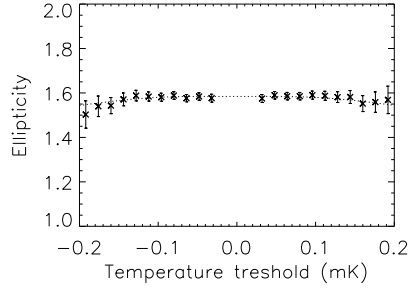
Fig. 2.— Number of spots in the V+W map as a function of threshold for a given size of spot. Data points are shown as crosses and the mean value from simulations as a dotted line. The confidence intervals are given to 2σ . Note that we only show the points for which we had sufficient spot statistics to be used in the analysis. Note also that the points are highly correlated.



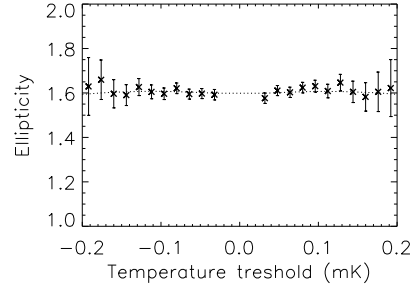
(a) > 3 pixel spots



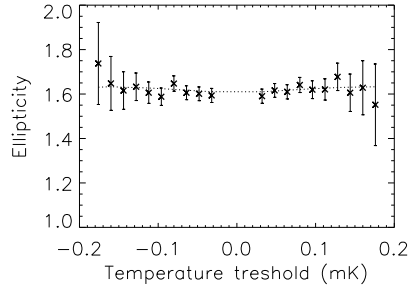
(b) > 8 pixel spots



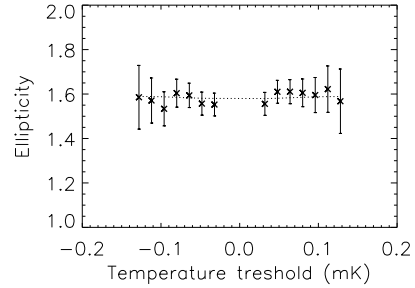
(c) > 20 pixel spots



(d) > 50 pixel spots



(e) > 100 pixel spots



(f) > 300 pixel spots

Fig. 3.— Spot ellipticity in the V+W map as a function of threshold for a given size of spot. Data points are shown as crosses and the mean value from simulations as a dotted line. Confidence intervals are given to 2σ . Note that we only show the points for which we had sufficient spot statistics to be used in the analysis. Note also that the points are highly correlated.

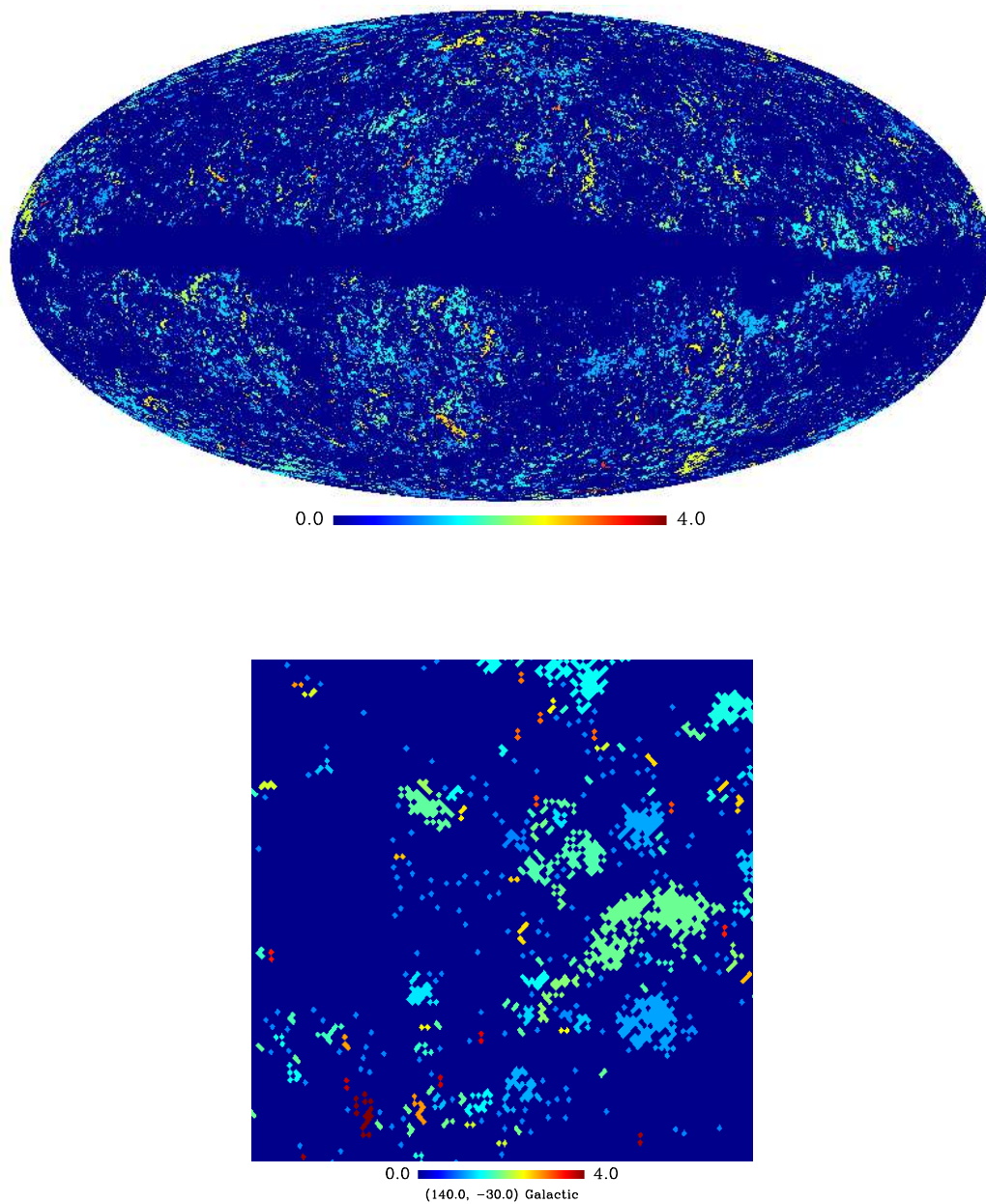


Fig. 4.— Color coded spot map for the V+W map with positive cut of $100\mu\text{K}$. Non relevant pixels have the value 0 and relevant pixels have value equal to their spots ellipticity. The zoom shows clearly some of the smaller spots having ellipticity of 4.0 or higher. Notice how two-pixel spots can have quite differing ellipticity depending on position as pixels are stretched to maintain equal area.

Table 1. VW band χ^2 expressed as percentage of simulated maps with *greater* χ^2 than the corresponding *WMAP* values.

Spot size	Number of spots	Ellipticity	Obliquity
> 3	74	20	15
> 8	73	13	29
> 20	43	82	42
> 50	20	10	79
> 100	67	22	44
> 300	25	81	90

Table 2. Q band χ^2 expressed as percentage of simulated maps with *greater* χ^2 than the corresponding *WMAP* values.

Spot size	Number of spots	Ellipticity	Obliquity
> 3	45	14	1
> 8	76	10	35
> 20	92	82	32
> 50	42	96	99
> 100	53	82	38
> 300	72	81	3

5. Discussion

The spots in this paper were defined in the same manner as Gurzadyan et al. (2003b), as was the formula for calculating ellipticity

$$\epsilon = \frac{a}{b} \tag{4}$$

for a and b as major and minor axis respectively. The definition of semi-major axis, however, was slightly different to the one presented in Gurzadyan et al. (2003a), where the semi-major axis is found by defining the spot center and letting the semi-major axis be the line to the center of the spot from the pixel furthest away from that center. This difference in calculation of semi-major axis should disappear when averaged over many spots and for sufficiently large spots the ellipticity should be close to the theoretical mean value of $\epsilon \approx 1.648$ (Aurich et al. 2010) in both cases. We have shown above that this is indeed the case for our algorithm, whereas in Gurzadyan et al. (2007) (Figure 7) the mean ellipticity for simulated maps is always above 2 for any pixel size. Note that our results are based on the 7-year release of the WMAP data, whereas Gurzadyan et al. (2007) used the 3-year release. Small differences in noise fluctuations between the two data releases will cause tiny differences in the absolute numbers for ellipticity, but this is unlikely to be the reason for the 10 sigma detection of excess ellipticity in Gurzadyan et al. (2007).

Obliquity was also calculated slightly differently, but here our results agree with Gurzadyan et al. (2003b) in that no significant detection could be found.

Residual foregrounds were not considered, and confidence was placed on the mask. The mask used (KQ85) is fairly liberal, and this may create problems especially in the Q band; if so, the effect is small enough not to be detectable.

In table 1 and 2 we presented χ^2 for ellipticity and obliquity for different spot sizes. In these table there are no indications for excess ellipticity or obliquity for any spot size. In order to check whether such numbers are

expected given the number of data points, we also calculated the total χ^2 taking into account all spot sizes. The results are shown in table 3 where we also show χ^2 values for the skewness and kurtosis of ellipticity and obliquity. All values seem to indicate that the ellipticity and obliquity of spots in the WMAP data are consistent with simulated data sets based on the concordance cosmological model.

6. Conclusions

Gurzadyan et al have, in several papers, claimed strong evidence for an abnormally high ellipticity in the hot and cold spots of CMB fluctuations as measured both by BOOMERanG and WMAP and to a certain extent also COBE (Gurzadyan et al. 2003a,b, 2005b). Here, the WMAP seven year data was examined in the Q, and combined V+W band maps to look for such an effect. No extraordinary ellipticity was found, and the results obtained here also disagree with the reported substantial difference in ellipticity for spots greater than 50 pixels compared to results when spots of 20 to 50 pixels also are included.

Gurzadyan et al. (2003a,b, 2005b) also reports that no preferred direction can be found to any statistical significance on the CMB spots. Our results agree that no such direction can be found to within a satisfactory statistical confidence.

Gurzadyan et al interpret the claimed ellipticity as evidence for geodesics mixing in a hyperbolic universe (see for instance Gurzadyan et al. (2005b)). This is contrary to reports suggesting that the universe is flat; first from BOOMERanG (De Bernardis. 2000), then from WMAP data (Spergel et al. 2007; Hinshaw et al. 2009) (with the latter reporting $-0.0179 < \Omega_k < 0.0089$ to 95% confidence) and also contrary to claims that no difference in ellipticity should be found even with substantial revisions of standard cosmological models (Aurich et al. 2010). Not detecting any abnormal ellipticity is thus consistent with the current cosmological standard model. This holds true for all frequency maps considered.

As the Planck mission will be releasing its data, redoing the analysis on higher resolution maps will determine the extent of pixel effects and noise in the heightened ellipticity for the smallest spots. Probing smaller scales will not only increase the statistics overall, but make it possible to compare ellipticity of large spots to small ones given the increased sensitivity. But with currently available WMAP data, we are not able to reproduce the results of excess ellipticity reported in previous papers.

FKH is thankful for a grant from the Norwegian Research Council. We acknowledge the use of the HEALPix package and of the Legacy Archive for Microwave Background Data Analysis (LAMBDA). Support for LAMBDA is provided by the NASA Office of Space Science. Support for HEALPix is provided by JPL at CalTech and the international HEALPix crew.

REFERENCES

- Aurich, R., Janzer, H. S., Lustig, S., & Steiner, F. 2010, arXiv:1007.2722
- Bennett, C. L., et al., 2003, ApJS, 148, 1
- De Bernardis, P., et al., 2000, Nature, 404, 69
- Gorski, K. M. et al., 2005, ApJ, 622, 759
- Gurzadyan, V. G., et al., 2003a, Int. J. Mod. Phys. D, 12, 1859
- Gurzadyan, V. G., et al., 2003b, Nuovo Cim., 118B, 1101
- Gurzadyan, V. G., et al., 2005a, Mod. Phys. Lett. A, 20, 491
- Gurzadyan, V. G., et al., 2005b, Mod. Phys. Lett. A, 20, 813
- Gurzadyan, V. G., et al., 2007, Phys. Lett. A, 363, 121
- Hinshaw, G., et al., 2009, ApJS, 180, 225
- G.F. Smoot et al., 1992, ApJ, 21, 1

Spergel, D. N. et al, 2007, ApJS, 170, 408

Table 3. total χ^2 summed over temperature threshold and pixel numbers expressed as percentage of simulated maps with *greater* χ^2 than the corresponding *WMAP* values.

Spot size	VW-band	Q-band
Number of spots	81	98
Ellipticity	6	27
Obliquity	13	2
Skewness ellipticity	46	1
Kurtosis ellipticity	13	49
Skewness obliquity	62	21
Kurtosis obliquity	60	58